Hydrothermal Oxidation: The Next Generation for Abatement of Unrecyclable Waste of Hazardous Nature and Complex Composition

B. Al – Duri[a*], F. Alsoqyani[a] and I. N. Kings[a]
[a] School of Chemical Engineering, University of Birmingham, Edgbaston, Birmingham B15 2TT, UNITED KINGDOM. Phone: +44(0)12141439
* B.Al-Duri@bham.ac.uk

ABSTRACT

Hydrothermal oxidation in supercritical water (SCW) is an advanced process that is highly effective for the treatment of unrecyclable waste organics frequently encountered in pharmaceutical, medical and chemical wastes. This work studied the enhancement of supercritical water oxidation (SCWO) of N-containing hydrocarbons namely DMF[1] and DBU[2]. Two approaches were adopted, namely multi-port oxidant injection, and addition of isopropyl alcohol (IPA) as co-fuel, respectively. Experiments were conducted in a continuous plug flow reactor system and results expressed in terms of TOC removal % and N-species yield %. Results showed that splitting a given oxidant dosage on two injection points improved TOC removal % depending on the oxidant injection locations and split ratio. However, it did not show a clear impact on N-speciation. On the other hand, addition of IPA facilitated oxidising recalcitrant aqueous ammonia (NH_4^+) towards N_2. Kinetic investigations using the *Global Power Law* were conducted and the activation energy (E_A), Arrhenius constant (k_o), and powers *a* and *b* were evaluated for all systems.

1. INTRODUCTION

More than 200 million people around the world are at the risk of exposure to hazardous waste. The World Health Organization, in conjunction with the World Bank, estimates that environmental risk factors contribute to more than 80% of regularly reported illnesses. Hazardous wastes arise from most industries, household, construction, medical practices, and mining, among many others. However in many industries the sludge remaining after treatment of wastewater accounts for much of the generated hazardous waste due to the uncontrolled potentially toxic elements (PTEs). If sent to landfill, not only would they damage the soil but also release hazardous chemicals into air and water. Thus the greatest concern with disposal of hazardous waste is landfill (or injection wells). Supercritical water oxidation (SCWO) is an advanced oxidation method, based on the special thermodynamic properties of supercritical water (SCW), where it becomes completely miscible with all organics (including polymers) and gases. In SCWO, complex hydrocarbons are oxidised in a homogeneous reaction medium, to CO_2, H_2O and salts, with >99% efficiency, no emissions of NO_x, SO_x or dioxins, and minimal ash. However, harsh environment inside the reactor and the insolubility of ionic compounds in SCW would lead to salt precipitation and corrosion, which have hindered the

[*] Corresponding Author.
[1] Dimethyl formamide
[2] 1,8 - Diazabicyclo[5.4.0]undec-7-ene

wide application of SCWO. N-containing organic wastes are abundant most hazardous wastes like pharmaceutical, clinical and household wastes. Upon degradation ammonia is released as a recalcitrant intermediate, which requires excessive temperatures and catalysts to be removed. This was the motivation behind selecting N-hydrocarbons for investigation. DMF is an amide, used in the production of acrylic fibres, plastics, and pharmaceuticals peptide coupling, among other applications. DBU is an amidine used in organics synthesis as catalyst, a complexing ligand and a non-nucleophilic base.

This work presents experimental and theoretical investigation of the enhanced SCWO process, using multi-port oxidant injection and IPA addition as co-fuel.

2. MATERIALS AND METHODS

2.1 Materials. Dimethyl formamide (C_3H_7NO) (Sigma-Aldrich, UK, 99%) and 1,8 - Diazabicyclo[5.4.0]undec-7-ene ($C_9H_{16}N_2$) (Sigma-Aldrich, UK, 99%), were the investigated organics. Isopropyl Alcohol (C_3H_7OH) (Sigma-Aldrich, UK, 99%) was the co-fuel, and aqueous hydrogen peroxide (Sigma-Aldrich, UK, 30wt%) was the oxidant.

2.2 Experimental Programme.

Fig. 1 is a flow diagram of the apparatus, described in previous works [1]. All studies were conducted in a 12m 1/16" SS316 plug flow reactor.

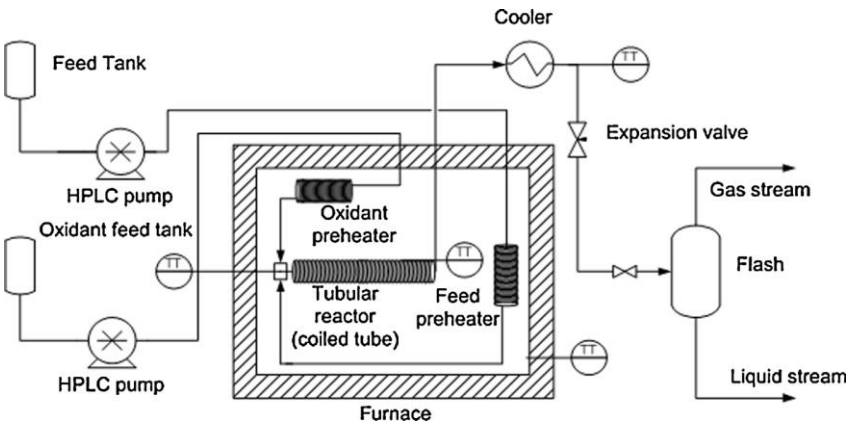

Figure 1. Process diagram of the laboratory scale SCWO apparatus

Study I- Multi-port split oxidant injection. 15 experiments were conducted for the SCWO of DMF at 400°C and 10mM initial concentration. A stoichiometric amount of oxidant (*1SR*) was split between two injection points situated at three different locations forming configurations *(a)*, *(b)* and *(c)* as shown in Fig. 2. For each configuration, five split ratios namely 75/25, 67/33, 50/50, 33/67, 25/75 were studied.

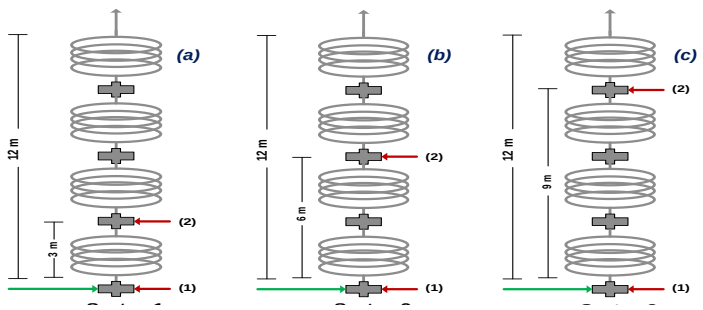

Figure 2. Primary (1) and Secondary (2) oxidants feed configurations (*a*), (*b*) and (*c*).

Study II – Co-fuel assisted system with IPA. SCWO of DBU was investigated under a range of temperatures, oxidant ratios, initial DBU concentrations, and $[IPA]_o/[DBU]_o$ molar ratios in a co-fuel assisted system. Table 1 shows the experimental range.

Table 1. Experimental system conditions

Variable	Range
Temperature, T (°C)*,**	400 - 525
Oxidant ratio, $nSR^{**,+,}$	0.8 - 2.0
Initial concentration, $[DBU]_o$ (mM)$^{+,*}$	1-10
$[IPA]_o/[DBU]_o$	0 - 4

$^{*}nSR=1$; $^{**}C_{DBU,o}=5mM$; $^{+}T=400°C$.

3. RESULTS

3.1 Study I - Multi-Port Oxidant Injection

The concept of multi-port oxidant injection was developed in 2005 [2] and proved to have several advantages: it distributed the quantity of oxygen along the reactor and improved the thermal control of the process by minimising hot spots. This work was conducted in an isothermal laboratory scale system and focused on the effect of splitting a given amount of oxidant over two injection points, on the conversion of organics and speciation of N.

Screening studies. Fig. 3 shows that under similar operating conditions, the TOC removal % is function of both the injection points and oxidant split ratio. In configurations (*b*) and (*c*), TOC removal was enhanced by 15 and 10% respectively. Gradual oxidant feed would imply lower oxidant flow rate (higher residence time), "regulated" free radicals release into the reaction stream and thus more efficient utilisation of oxidant, leading to better conversion and more controllable energy release. Configuration (*a*) did not show distinctive improvement over single oxidant feed, and was attributed to the fact that relatively short reactor length between the two injection points was not sufficient to allow the development of the radical pool. Therefore, it is recommended that oxidant ports are separated by distance long enough to allow release and development of free radicals.

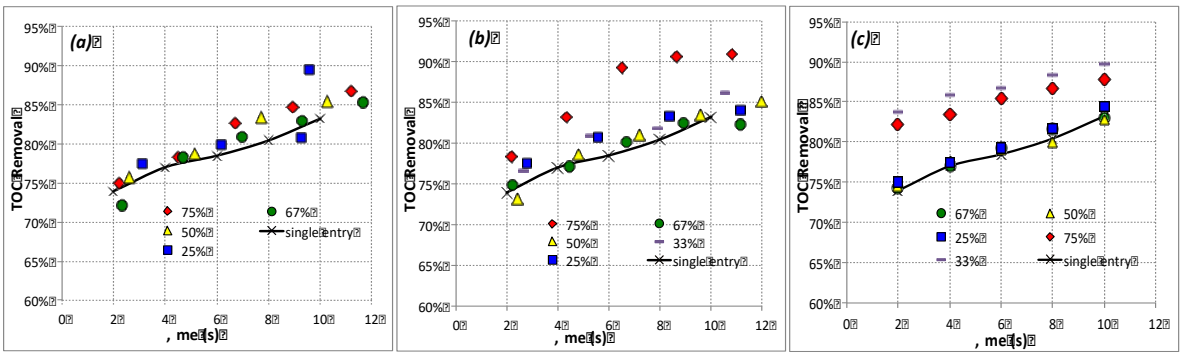

Figure 3. TOC removal % for configurations *b* (*3a*) and *c* (*3b*), at *1SR*, 400°C, $[DMF]_o$=10mM.

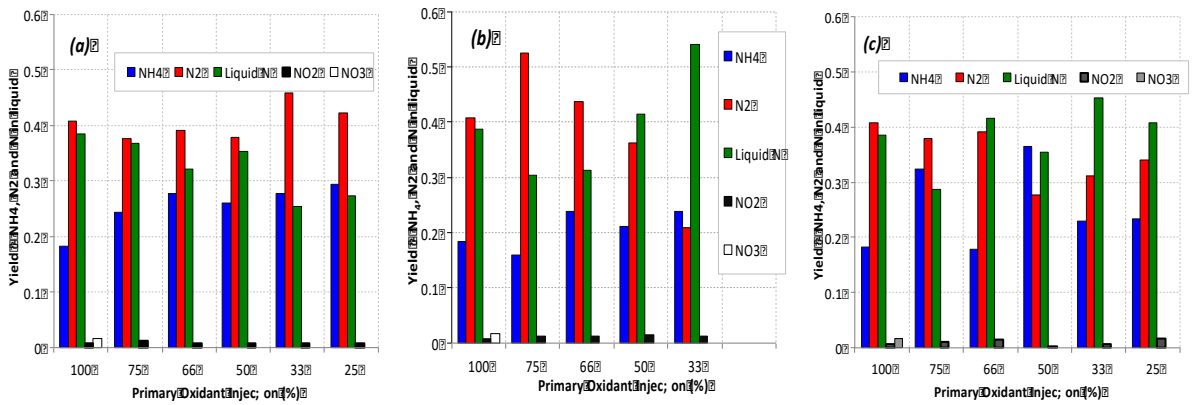

Figure 4. Yield of N-species N_2, NH_4^+, NO_3^-, NO_2^- and liquid N, in configurations *b* (*4a*) and *c* (*4b*).

Multi-port oxidant injection systems did not show a clear impact on N speciation (Fig. 4). Given that the oxidant dosage was <1SR in the first segment of the reactor, it implied that there was not sufficient oxidant to further oxidise TN (predominantly NH_4^+) to N_2. Overall, tendency towards NH_4^+ and/or N_2 was observed. However, 400°C was generally not sufficient for effective N oxidation.

System Kinetics. The system kinetic behaviour was modelled as two reactions in series:

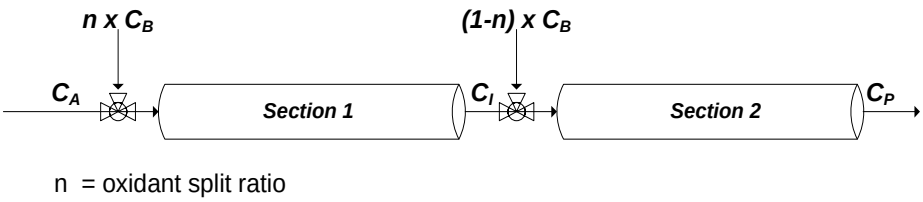

Figure 4. Conceptual diagram of the plug-flow reactor with two oxidant injection points

$$A + B_1 \overset{k_1}{\rightarrow} I \qquad (1)$$

$$I + B_2 \overset{k_2}{\rightarrow} P \qquad (2)$$

Where *A* is DMF, *B* is oxygen, *I* represent the intermediates, and *P* is the products. Based on the above, the reaction rate expressions follow the form of two successive reactors in series:

$$r_1 = \frac{dC_A}{dt} = -k_1[C_A]^a[C_{B1}]^b \qquad (3)$$

$$r_2 = \frac{dC_B}{dt} = -k_1[C_A]^a[C_{B1}]^b - k_2[C_I]^i[C_{B2}]^b \qquad (4)$$

$$r_3 = \frac{dC_I}{dt} = k_1[C_A]^a[C_{B1}]^b - k_2[C_I]^i[C_{B2}]^b \qquad (5)$$

$$\text{at } t = 0: m_{B1} + m_{B2} = m_B;\ m_A = m_{A0};\ m_P = 0 \qquad (6)$$

m_s is the number of moles of any species *s*. $[C_I]$ would be the output of *section 1*, which would combine with $[C_{B2}]$ to form the inputs to *section 2* in Fig. 4. Due to the lack of data required to complete the mass balance, it was not possible to solve the above equations. However, the *Global Power Law* was applied to predict the DMF removal rate taking into account the supplemental dilution effect of additional oxidant solution. As a starting point, *section 1* and *2* were assumed to be two single-oxidant entry plug-flow reactors, hence the same reaction constants evaluated for single-entry oxidant system (Eq. 7) were used for both sections, and the model was solved by Matlab program [3]:

$$\frac{d[DMF]}{dt} = 4.35\ x\ 10^{10} exp\left(\frac{-131{,}926}{RT}\right)[C_{org}]^1[O_2]^{0.6} \qquad (7)$$

Fig. 5 is the parity plot to compare experimental and calculated data:

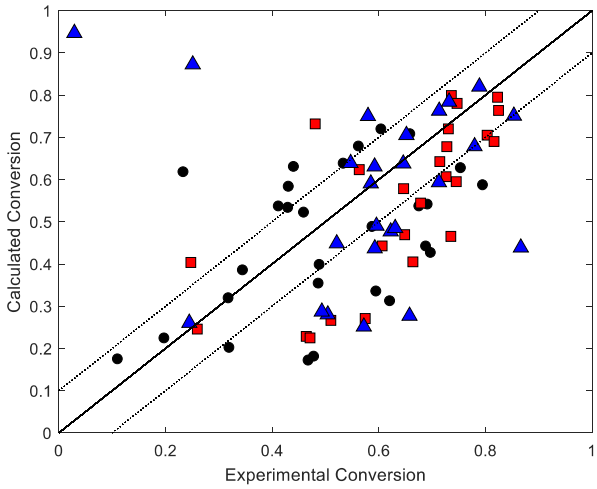

Figure 5. Parity plots for modelling configurations (*a*) (●), (*b*) (■) and (*c*) (▲).

Expectedly, experimental data deviated from the single-entry kinetic model. This was attributed to the different radical dynamics and additional radial mixing zones introduced by the secondary oxidant. The radical dynamics will be changed by the sudden influx of O_2 and hydroxyl radicals disrupting any steady state that might have formed. New species would be formed by drastically increasing the local OH• concentration (and thus the local reaction rates), and facilitating decreasing intermediate species (tri-, di, methyl amines, methanol…) whose consumption relies on local OH•. Experimentally the desired effect of oxidant splitting was achieved (Fig. 3), and a positive deviation is observed in Fig. 5. In other words, when a given amount of oxidant is distributed over two entries, the system performs better although it operates at an oxidant-deficient mode for the first part of the reactor. Modelling of such system kinetics requires the experimental data to close the material balance on all *C* species.

3.2 Study II - Co-Fuel Assisted SCWO

Results of this study discuss the effects of operating conditions namely temperature; initial DBU concentration; *nSR* and $[IPA]_o/[DBU]_o$ ratio, on TOC removal % and N yield % for the liquid phase. When oxidised, IPA generates radicals like HO•, HO_2•, $[CH_3COHCH_3]$•, CH_3•, and $[CH_3CHOHCH_2O_2]$•, which target the C-N and N-H bonds [4].

Effect of Temperature. Fig. 6 is a comparative plot of TOC removal and N yield % in IPA and IPA-free systems with respect to temperature, at *1SR*. Typically TOC removal % increased with temperature. The addition of IPA improved TOC removal by around 2.8 – 3% over the investigated temperature range, more significantly at lower temperatures and shorter residence times. As for N-species, total liquid nitrogen (TN) and aqueous ammonia (NH_4^+) yields % resembled quartic pattern: they increased slowly with temperature, showing higher increase above 475ºC, signifying further organics degradation at higher temperatures. As Fig.6b shows, upon IPA addition, both TN and NH_4^+ yield decreased by 25 – 30%, which confirmed the affinity of IPA free radicals towards N bonds. Lower yield% of TN and NH_4^+ implies that it was converted to N_2. However, at higher temperature more NH_4^+ was released by DBU oxidation, than was further oxidised to N_2. Possibly *1SR* was not sufficient at higher temperatures. Nitrates (NO_3^-) yield % was generally low. It remained <10% and diminished at 525ºC.

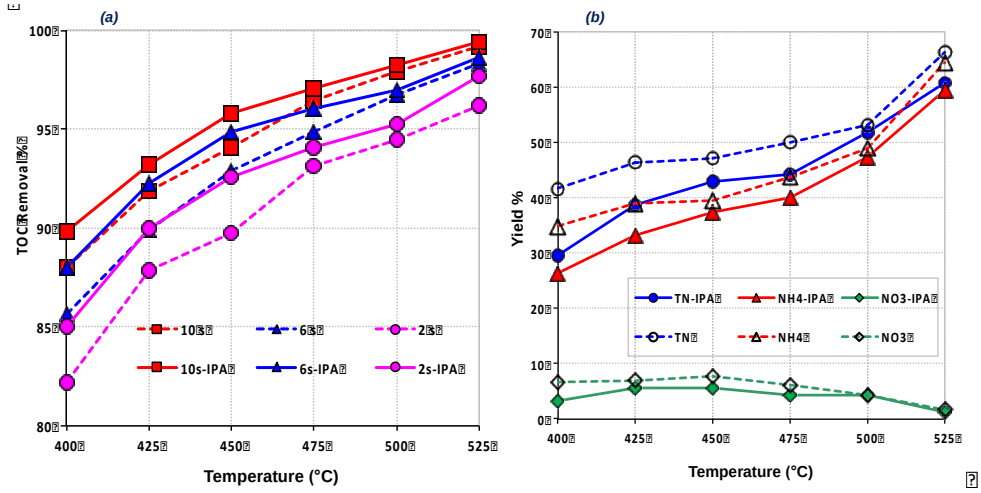

Figure 6. Effects of temperature on (a) TOC removal % and (b) total nitrogen (TN), ammonium (NH_4^+) and nitrate (NO_3^-) yields %, at 400ºC, $[DBU]_0$ = 5mM, 1 *SR*, [IPA]/[DBU] = 1.

Effect of SR. Fig. 7 illustrates the influence of combined IPA addition and oxidant, even at the relatively low temperature 400°C. The yield % of TN and NH_4^+ were lowered, in favour of conversion to N_2 gas: NH_4^+ decreased by 37% and 26% for *nSR* values of 0.8 and 1.0 respectively. Similarly, TN decreased by 31% and 30%, respectively. This confirms the influence of free radicals released by IPA interact with the N species and result in further oxidation. However, temperatures higher than 400°C would help achieve better conversions.

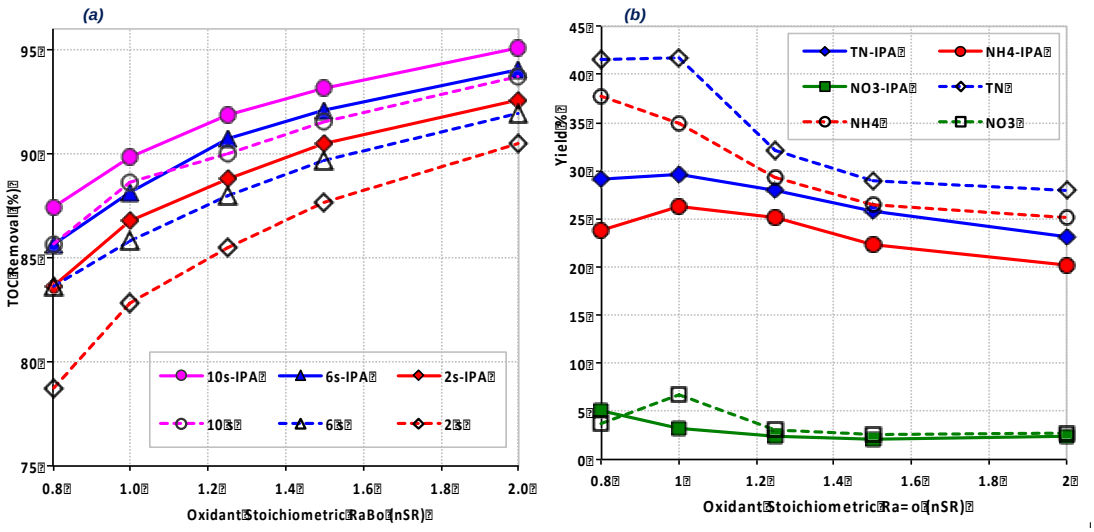

Figure 7. Effects of *nSR* on (a) TOC removal % and (b) total nitrogen (TN), ammonium (NH_4^+) and nitrate (NO_3^-) yields %, at 400ºC, $[DBU]_o$ = 5mM and $[IPA]_o$ /$[DBU]_o$ = 1.

Kinetic Studies. The *global rate expression* was applied to evaluate the SCWO rate constants merging both DBU and IPA as organics therefore the rate equations were expressed in terms of [TOC][5]. Eq. (8) and (9) recap the rate expressions for IPA-free and IPA systems respectively:

$$\frac{d[TOC]}{dt} = 1.79x10^2\ exp\left(\frac{-46{,}703}{RT}\right)[TOC][O_2]^b \qquad (8)$$

Where $b=0.097$ for $[O_{2,o}] \leq 1SR$, and $b=0.299$ for $[O_{2,o}] \geq 1SR$.

$$\frac{d[TOC]}{dt} = 8.5x10^2\ exp\left(\frac{-56{,}638}{RT}\right)[TOC][O_2]^{0.534} \qquad (9)$$

The varying value of *b* values demonstrate different dependence on $[O_{2,o}]$ between the oxidant-deficient and oxidant-rich conditions. At low oxidant dosages, fewer free radicals (HO• and HO_2•) would be released, and thermal degradation is suggested to dominate the reaction as opposed to free radicals, forming nitro groups that drive SCWO [6]. This could obscure the influence of oxygen, giving rise to an almost *zero* order. However, more detailed pathway investigations are required to confirm the hypothesis. For *nSR* > *1.0* the value of *b* is within the range of other works [7]. Also the reaction rate constant increased by almost fourfold, proving the positive influence of IPA. Coexistence of IPA and DBU does enhance SCWO of both species due to the formation of extra free radicals propagating a chain reaction, enhanced by the nitro groups formed due to DBU-IPA interaction [8].

Supercritical Water Oxidation of NH_4^+ as feedstock. In order to focus on ammonia as a particular recalcitrant, the influence of IPA on SCWO of NH_4^+ as feedstock was investigated. TN analysis were carried out at all residence time while NH_4^+ analysis were done at *t*=6s. SCWO of aqueous ammonia was conducted at several *T* and *nSR* values, and the results in Figs. 8a and 8b show great improvements: At 550°C and *1SR* NH_4^+ removal reached 85%, while the same value was achieved at 450°C when *nSR* was 1.5, as shown in Figs. 8a and 8b, respectively.

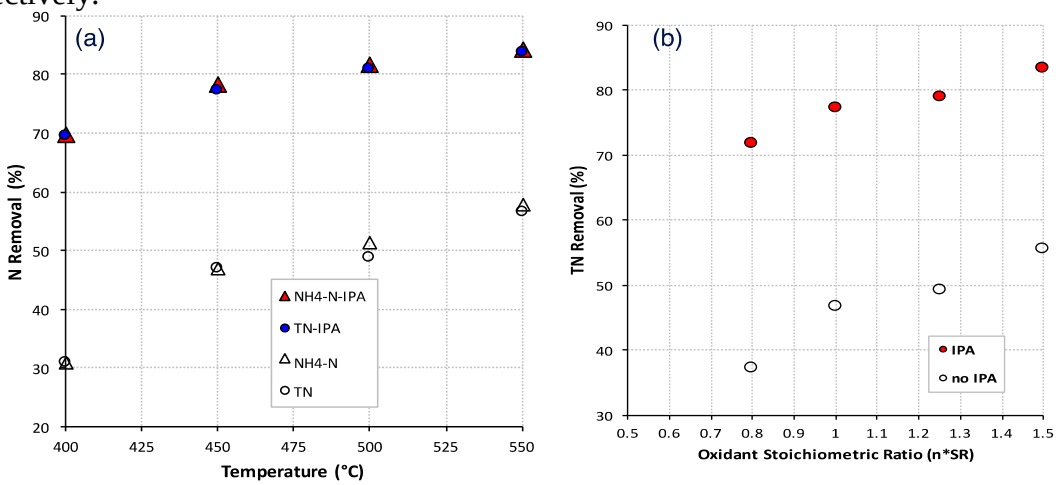

Figure 8. Effects of (a) temperature on TN and NH_4^+ removal % at *nSR* = 1, and (b) *nSR* at temperature = 450°, on TN removal %. All at $[NH_4^+]_o$ = 10mM, and $[IPA]_o/[NH_4^+]_o$ = 1.0, and *t=6s*.

The presence of alcohol in ammonia oxidation allows for the occurrence of HO_2• reactions with alcohols that produce H_2O_2 during the early stages of oxidation through the hydrogen abstraction reactions, which in turn generates more radicals of HO_2• and HO• radicals [4].

Effect of IPA/feedstock Ratio. Increasing the $[IPA]_0/[NH_4^+]_0$ ratio on % N removal, when ammonia is an intermediate of DBU oxidation and when used as feedstock is shown in Fig.9. It shows that 98% ammonia removal was achievable at 450 °C when IPA/NH_4^+= 4. This is indeed a promising outcome in terms of solving the problem of ammonia in industrial aqueous effluents. On the other hand, although N removal from DBU feedstock was improved, it did not exceed 80%. It suggests that under the experimental conditions, IPA might use much oxidant before ammonia is released. Therefore, it is advisable to feed the IPA at more than one injection port in N-containing hydrocarbon systems.

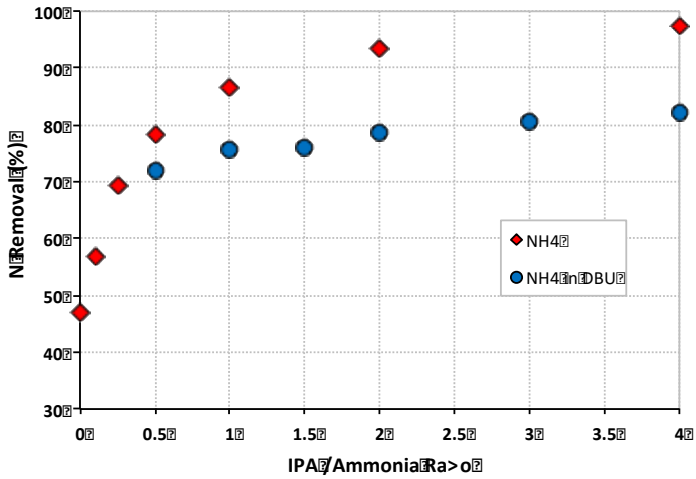

Figure 9. Effect of [IPA]/[feedstock] ratio on NH_4^+ removal %, as feedstock and intermediate.

To quantitatively describe the ammonia removal, the *pseudo-first order* approximation was followed with respect to N. For the analysis, it was assumed that IPA and oxidant were both in excess, and a *zero* order with respect to both respectively was assumed. Eq. (6) is the first order approximation for the change of (NH_4^+) with time. To quantitatively describe the ammonia removal, the *pseudo-first order* approximation was followed with respect to N. For the analysis, it was assumed that IPA and oxidant were both in excess, and a *zero* order with respect to both respectively was assumed.

$$ln\left({[TN]}/{[TN]_0}\right) = k_0 exp\left({-E_a}/{8.31T}\right) t \quad (10)$$

Where k_0 values are *0.375* and *3.64* s^{-1} for NH_4^+ and (NH_4^++IPA) systems, respectively. E_A values are *22,245* and *52,064* $Jmol^{-1}$ respectively.

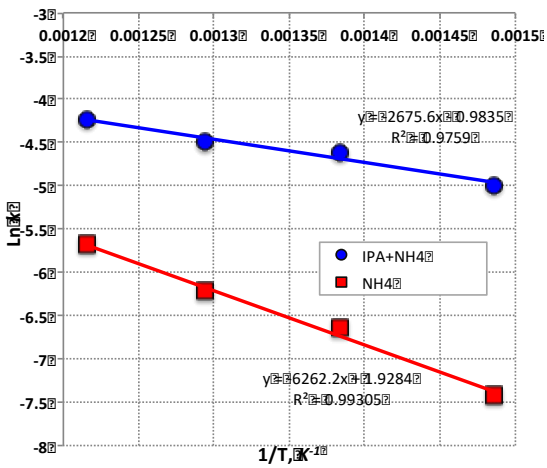

Figure 10. Arrhenius plots for SCWO of NH_4^+ and NH_4^++IPA systems.

Fig.10 shows that IPA addition had a significant influence on the reaction rate constant *k* (in terms of E_A and k_0). IPA addition greatly enhanced the rate of NH_4^+ oxidation. This is attributed to the high heating value of IPA ($\Delta H^{Ø}$ = 2021 kJ mol^{-1}), and the rapid release of extra free radicals, which propagated a chain free radical reaction.

4. CONCLUSIONS

Study *I* demonstrated that multi-port oxidant injection improved TOC removal % to an extent, which depended on the split ratio and injection points. Study *II* showed that removal recalcitrant aqueous ammonia upon SCWO of N-containing hydrocarbons can be significantly improved by addition of IPA. Multi-port IPA injection is recommended, as fresh IPA has better impact of free NH_4^+ as opposed to residual ammonia.

5. REFERENCES

[1] AL-DURI B. *et al.*, *Philos. Trans. R. Soc.* A, 2015, 373: 20150013.
[2] CANSELL F., U.S. Patent No. 6929752B2; 2005.
[3] KINGS I.N., PhD thesis, University of Birmingham, UK, 2013.
[4] ZHONG J. *et al.*, *J. Fuel Chem. & Technol.*, 2014, **42**(3), 343.
[5] AL-DURI B., ALSOQYANI F., *J. Supercrit. Fluids*, 2017, **128**, 412.
[6] WANG Q. *et al.*, *Desalin. Water Treat.* 2013, **51**(37-39), 7025.
[7] WEBLEY J.W. *et al.*, *Ind. Eng. Chem. Res.*, 1991, **30,** 1745.
[8] LI X., *et al.*, *Chem.*, 2012, **77**(4), 1722.